

# Late Cenozoic shelf delta development and Mass Transport Deposits in the Dutch offshore area – results of 3D seismic interpretation

A. Benvenuti<sup>1,3,4,\*</sup>, H. Kombrink<sup>1</sup>, J.H. ten Veen<sup>1</sup>, D.K. Munsterman<sup>1</sup>, F. Bardì<sup>2</sup> & M. Benvenuti<sup>3</sup>

1 TNO – Geological Survey of the Netherlands, P.O. Box 80015, 3508 TA Utrecht, the Netherlands.

2 DataCo Ltd, Den Haag, the Netherlands. England Head Office: DataCo Ltd, Townend, Shootersway Lane, Berkhamstead, Herts, United Kingdom, HP4 3NW.

3 Earth Science Department, University of Florence, Via La Pira 4, 50121 Florence, Italy.

4 Present address: Department of Geology and Paleontology, University of Geneva, Rue des Maraîchers 13, CH-1205 Geneva, Switzerland.

\* Corresponding author. Email: antonio.benvenuti@unige.ch.

Manuscript received: February 2012, accepted: August 2012

## Abstract

In this study, seismic stratigraphic criteria have been used to characterise the evolution of the Southern North Sea (SNS) shelf-delta system that progressively filled the Southern North Sea basin during Plio-Pleistocene times. Based on the prograding and down-stepping architecture of the shelf-delta sequence it is inferred that deposition occurred during a time of high sediment supply and overall sea-level lowering. During this time the delta slopes failed several times, creating at least 30 internally coherent Mass Transport Deposits (MTDs) mainly grouped in common areas, affecting the same clinoform set and partially sharing the basal shear surface (groups of MTDs). The most important features of the studied MTDs are 1) the dominance of brittle deformation; 2) the small amount of material removal from the headwall domain (lack of completely depleted areas above the basal shear surface); and 3) the lack of an emergent toe domain above the un-failed sediment located basinward, although proper confining geometries for the MTD are not detected. Therefore, the studied MTDs can neither be classified as frontally confined nor as frontally emergent but they are a new intermediate type of submarine landslides which has not been described before. These characteristics suggest that the mass movement ceased relatively soon after initiation of failure. Incisions on top of the MTDs suggest the presence of erosive flows. These flows were probably generated due to a concentration of the drainage in the negative morphology the failure event left behind in the upper sector of the slope. The stronger progradational character of the reflections on top of MTDs confirms a concentration of drainage after the erosional phase too.

The interplay between high sediment supply and constant or even decreasing accommodation space (caused by constant or decreasing sea-level) is supposed to be the main precondition for slope instability for most of the MTDs in this study area. Slope failures themselves can also be considered a preconditioning factor by the creation of local very high sedimentation rates (see groups of MTDs). Salt-induced seismicity and storm waves' effect superimposed on high frequency sea level fall are considered the most important triggering factors.

**Keywords:** Mass transport deposits, Eridanos delta, sequence stratigraphy, Plio-Pleistocene

## Introduction

Deposits of the Southern North Sea (SNS) shelf-delta system, also called Eridanos Delta System (Overeem et al., 2001), represent an important succession in the Late Cenozoic stratigraphy of the SNS. Prograding clinoforms gradually filled in the SNS basin from the east-northeast with mainly clayey to silty sediments,

coarsening up to sands in the upper part. Sørensen et al. (1997) detected up to 45 sequences in the whole SNS by using 2D seismic sections and well-log data. Many studies address the sedimentary evolution of the SNS shelf-delta system (Cameron et al., 1993; Sørensen et al., 1997; Michelsen et al., 1998; Overeem et al., 2001; Huuse & Clausen, 2001; Huuse, 2002; Kuhlmann, 2004; Kuhlmann et al., 2006; Kuhlmann & Wong, 2008) and much

is known about variations in direction of progradation, age of sediments and regional sequence stratigraphic development. The increasing availability of 3D seismic data over the last decade enables the smaller-scale architecture of the delta system to be studied as well.

Here, high resolution 3D seismic data have been used to study the deltaic succession in the eastern sector of the Dutch North Sea (G, M and eastern part of the F quads; Fig. 1). Detailed mapping of the Neogene-Quaternary succession revealed a complex set of slope failures associated with individual delta clinoform sets within the delta system. Slope failure is one of the most important sediment transport mechanisms forcing large amounts of sediment to move downslope (Hampton et al., 1996; Lucente & Pini, 2003; Canals et al., 2004; Bull et al., 2009). Submarine slope failures occur in various geological settings and can easily incorporate sediment volumes two or three orders of magnitude greater than subaerial landslides (Hampton et al., 1996). The biggest submarine landslide reaches 20,000 km<sup>3</sup>

(Agulhas Slide in South Africa) while the biggest subaerial landslide encompassed a few km<sup>3</sup> only (26 km<sup>3</sup> the Mount Shasta landslide; Hampton et al., 1996). They are very common in tectonic active areas, but also occur in numerous tectonically quiet settings. Fjords, active river deltas on the continental margin, submarine canyon-fan systems, open continental slopes and oceanic island flanks and -ridges are the areas where slope failures mostly occur (Hampton et al., 1996), especially where the slope consists of fine-grained sediment (Masson et al., 2005). In the absence of seismic triggers, such as on passive margins, climate can play an important role in the timing of slope failure. On glaciated margins they are common during the transition from a glacial to an interglacial period due to the isostatic rebound of the continental margin as a consequence of ice-sheet melting. On non-glaciated margins they are instead more common during glacial periods due to a strong increase of sediment supply (Lee, 2009; Leynaud et al., 2009).

Stacked slope failures or Mass Transport Deposits (MTDs) have been mentioned in the study area before (Cameron et al., 1993; Sørensen et al., 1997; Overeem et al., 2001) but they had not been mapped in detail using 3D seismic data. The main aims of this paper are to present: 1) the characteristics of the MTDs based on an extensive study in which the internal and external geometries of the MTDs have been investigated; and 2) to place the occurrence and features of the MTDs in a depositional model that describes the development of the delta system.

## Geological setting

The Cenozoic North Sea Basin is an intracratonic sag basin, overlying the failed Mesozoic North Sea rift system (Ziegler, 1990). In cross-section, the Cenozoic sedimentary succession in the North Sea Basin displays a saucer shape where the depocentre (>3 km of sediments) corresponds to the axis of the Jurassic-Cretaceous graben system. The Paleogene succession in the Southern North Sea reflects deposition in a shallow marine environment, where inversion and associated uplift of the former graben areas intermittently prevented sedimentation (De Jager, 2003; De Lugt, 2007). From Oligocene to Pleistocene times, the eastern North Sea Basin was filled by deltaic and pro-deltaic sediments supplied progressively from the N, NE, E and SW (Michelsen et al., 1998; Huuse, 2002). Following a period of sediment starvation (Mid-Miocene Unconformity), an important phase of deltaic sedimentation in the Dutch sector of the North Sea started in Pliocene times. Major clinoforms, propagating from Denmark towards the west, caused sedimentation rates to increase abruptly (Cameron et al., 1993; Sørensen et al., 1997; Overeem et al., 2001; Huuse, 2002). At that time, sediment supply was dominated by a very extensive and wide fluvio-deltaic river system: the Baltic river system (Bijlsma, 1981). The drainage area comprised the Fennoscandian and Baltic area and was comparable with the largest present-day deltaic systems (Overeem et al., 2001).

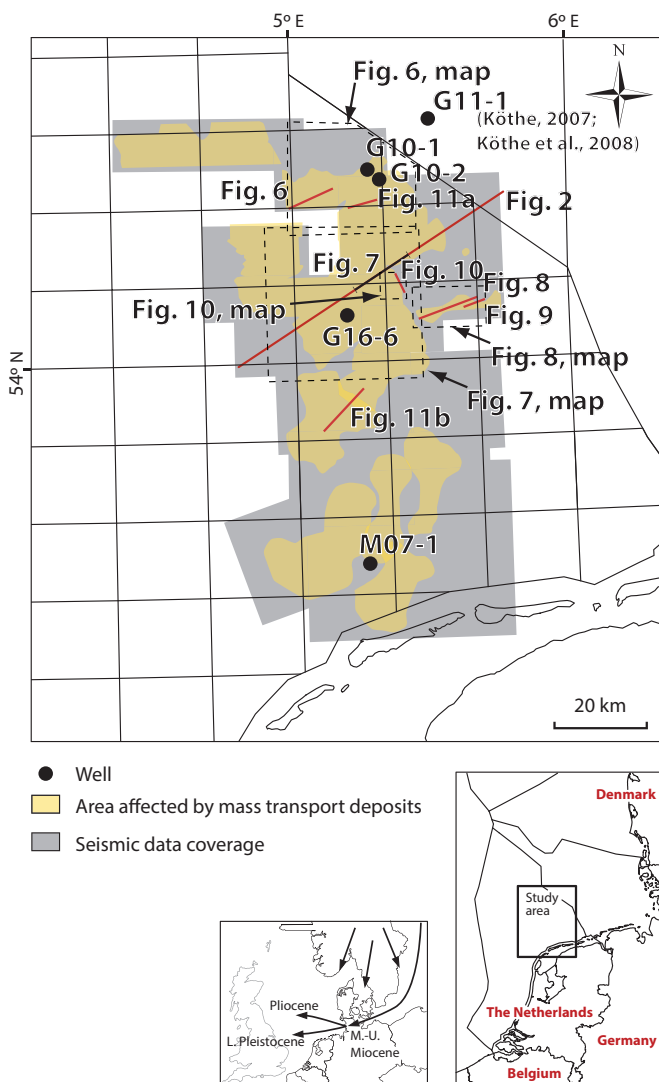


Fig. 1. Location of study area and studied surveys in the eastern sector of the Dutch offshore, in the Southern North Sea. The study is entirely based on high resolution 3D seismic volumes (in grey).

The Mid-Miocene Unconformity (MMU) forms the base of the succession studied in this paper. The MMU forms the best seismic marker in the Neogene succession in the Southern North Sea. In fact, this unconformity represents, at a large scale, a slope profile (clinoform) and associated basinal and landward continuations that experienced sediment starvation for a long time (Huuse & Clausen, 2001). On seismic data from offshore Denmark, this period of sediment starvation is evidenced by the presence of scarps immediately basinward of the clinoform breakpoint (Huuse & Clausen, 2001). In the study area, the MMU forms the basinward continuation of the clinoform further to the east and therefore appears as a horizontal surface. Toward the west the MMU shallows and shows an overall eastward dip.

The MMU and the under- and overlying sediments caused quite some debate as far as their forcing mechanisms are concerned. The sediments immediately below the MMU were deposited by an Early to Middle Miocene shelf delta system which was prograding to the SW. The easternmost Danish North Sea formed the depocentre at that time. In Langhian times, a transgression (Hodde transgression) led to the establishment of marine depositional conditions in Denmark and a period of sediment starvation in many parts of the eastern North Sea. Following a hiatus of several millions of years, delta sedimentation resumed again at very high rates. The transport direction had changed from NE-SW to E-W, which caused northern Germany to become the new depocentre. The overall progradation of the delta is reflected by the onset of sedimentation onto the MMU (Huuse & Clausen, 2001). This age is estimated at 14–15 Ma for the Danish offshore sector (Huuse & Clausen, 2001), at 10.7 Ma for the German sector and at 11.2 Ma for the southern Norwegian sector (Eidvin et al., 1999). An early Late Miocene age is given by Köthe et al. (2008) in borehole G-11-01, located very close to the study area.

Rasmussen (2004) mentions that the Hodde transgression cannot be directly correlated to a climatically controlled glacio-eustatic sea-level change and proposes a combination of both climatic variation and tectonic activity. The formation of a dome in SE Scandinavia (Japsen & Bidstrup, 1999) is suggested to be the cause of both the cessation of sediment input and the rotation of transport direction (from SW to W; Rasmussen, 2004). In contrast, Huuse & Clausen (2001) question the hypothesis of tectonic uplift of southern Norway. Huuse (2002) and Huuse & Clausen (2001) link the transgression to a minor eustatic sea-level rise. The subsequent shift to westward progradation

is suggested to relate to large scale autocyclic behaviour or renewed inversion of the Sorgenfrei-Tornquist Zone (Huuse et al., 2001). The increase in sediment supply in Late Miocene times is explained by global deterioration in climate, which caused sediment supply to increase in many places (Huuse & Clausen, 2001). Rasmussen (2004) and Rasmussen (2009) state that climate did not have a major influence on sediment supply because high sediment supply has both been found in cool as well as subtropical climates. From the Gelasian onward however, it has been clearly shown by Kuhlmann et al. (2006) that glaciations and thus climate fluctuations did play an important role in variations of sediment supply and grain size in the Southern North Sea. Therefore, the shelf delta development described in this paper is linked to glaciations in the Late Pliocene-Pleistocene.

## Data and methods

### Data analysis

High resolution 3D seismic surveys have been used to study the MTDs and the delta architecture (Table 1 and Fig. 1). The in- and crossline spacing is 25 m while the sampling rate is 4 ms. The vertical resolution of the data for the studied interval is roughly 13 m. The interpretation was carried out in Petrel (Schlumberger, version 2009.2). The use of time slices allowed detailed mapping of the direction of progradation of the delta clinoforms and the presence and shape of erosional features affecting particular reflectors. The amplitudes have been analysed in black and white in order to better visualise the geometries of the reflectors, especially the internal geometry of the MTDs. The variance (or coherency) attribute also helped identify erosional features and (the outlines of) MTDs on time slices. The variance attribute shows the degree of continuity of seismic amplitudes from one trace to the other. Chaotic seismic facies, usually characterised by rapidly changing amplitudes, are well recognisable in a variance cube. Specific MTD-geometries like headwall scars, extensional ridges and blocks in the headwall domain and other important indicators of MTDs could be well identified too. Each MTD has been defined on 3D seismic data by mapping the base (basal shear surface) and top of the deformed unit. In order to better analyse the mapped surfaces, the variance and amplitude have been plotted on these surfaces. Volume and thickness of each MTD as well as the height and the dip angle of the clinoforms

Table 1. Seismic volumes and well data (logs and captions) used for this study.

Seismic dataset					
Z3WES2003A	Z3PET1994A	PET1991A	Z3NAM1997A	NAM1993C	Z3CLY1998A
Z3NAM1990E	Z3NAM1991A	Z3NAM1991D	Z3PET1991B	Z3NAM1994A	Z3NAM1996A
Well data					
G10-1	G10-2	G16-6	M07-1		
(captions + logs)	(captions + logs)	(logs)	(logs)		

were calculated using a seismic velocity of 2000 m/s, following Cameron et al. (1993) and Storvoll et al. (2005). This velocity agrees with available checkshots of the well log G-10-01.

### Seismic stratigraphy

The deltaic succession has been interpreted in terms of the seismic-stratigraphic criteria presented by Catuneanu et al. (2009) and subdivided in depositional sequences characterised by different stratal stacking patterns (system tracts). The depositional sequences are bounded by unconformities and correlative conformities (c.f. Catuneanu, 2006) taking into account the scheme proposed by Hunt & Tucker (1992).

Variations in stratal stacking patterns are mainly the result of different ratios between the rate of creation of accommodation space ( $A'$ ) and sedimentation rate ( $S'$ ), which are not exclusively influenced by sea-level fluctuations. In delta systems the autochthonous shifting of prograding lobes, which are not related to relative sea-level fluctuations, may also induce lateral differences in the  $A'/S'$  ratio and thus affects the stratal architecture as well. The identification of the clinoform break point trajectory in seismic data, which usually approximates the shoreline trajectory, might result in a clearer link between changes in stratal architecture and sea-level fluctuations (c.f. Helland-Hansen & Martinsen, 2008).

In order to link the occurrence and timing of the mass failures to the seismic-stratigraphic architecture, the deltaic succession has been subdivided in 3 lower order genetic units. Each unit reflects a stratal package with different types of MTDs. In turn, these units consist of depositional sequences that reflect higher-order accommodation changes (Fig. 2).

### Mass Transport Deposits (MTDs): description and interpretation

MTD is a general term to identify deposits affected by submarine slope failure without implying a particular style of mass movement. MTDs can be associated with several geometries and seismic facies depending on the kind of mass movement (Mulder & Cochonat, 1996). The kinematic indicators described in the review of Bull et al. (2009) have been used for MTD identification and characterisation of internal and external geometries (Fig. 3). The relative timing of the MTDs has been reconstructed by analysing the spatial distribution of the headwall scars and their cross-cutting relationships with affected strata. MTDs have been grouped where they are part of a complex of (partly overlapping) failures. The relative chronology of each mapped group has also been established by the identification of the clinoform in which the headwall scar terminates in upward direction.

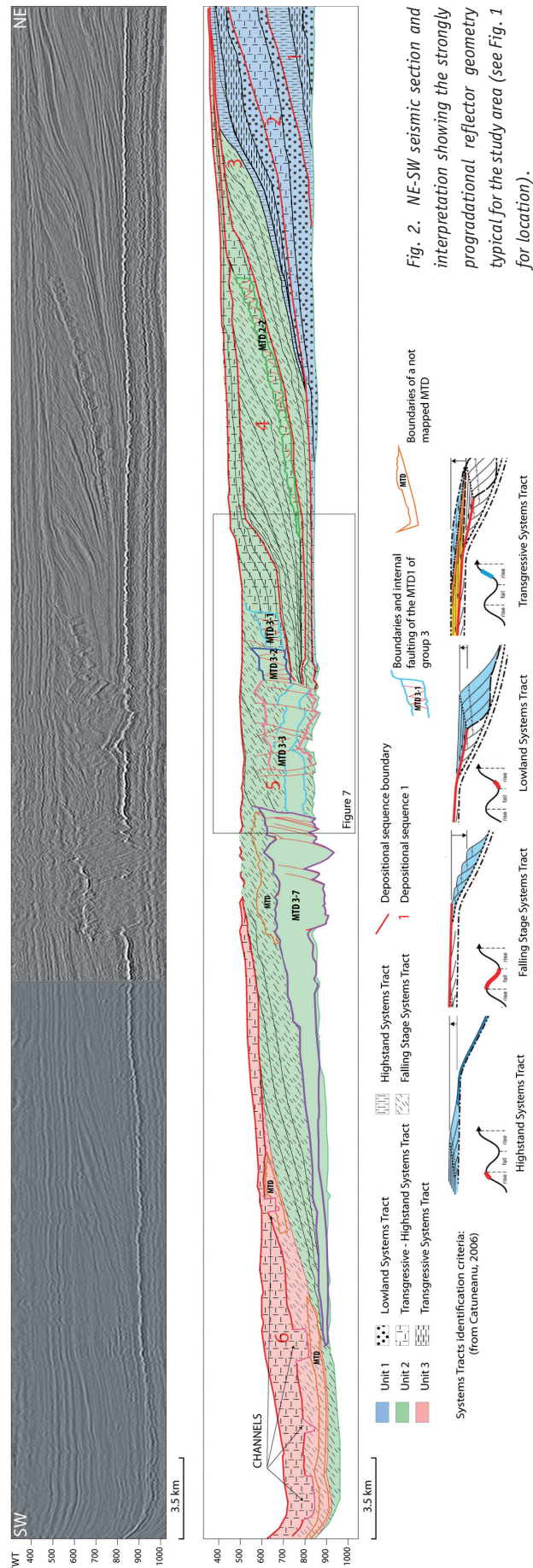
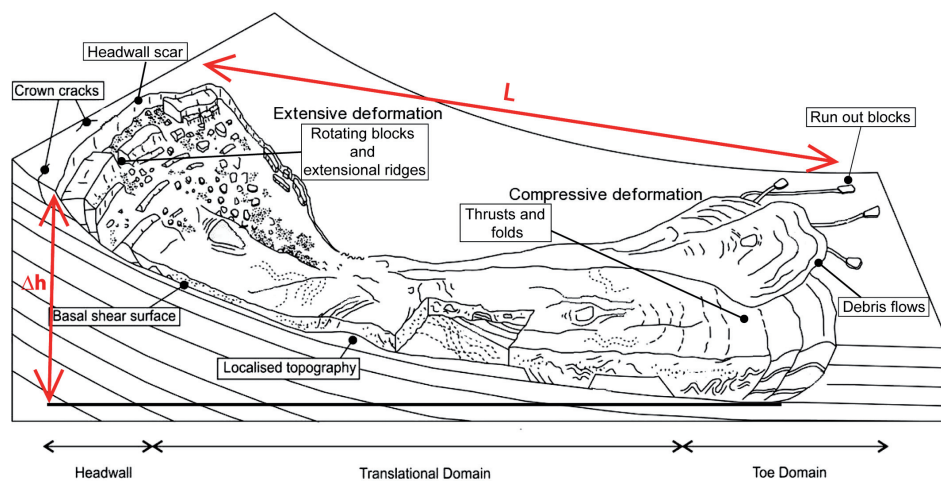


Fig. 3. Schematic representation of a MTD, showing typical domains, features and structural expressions. Extensive deformation is typical of the headwall domain where rotating blocks and extensional ridges dominate; compressive deformation is typical of the toe domain where thrusts and folds dominate. The translational domain can be either not deformed or consist of a mix of both extensional and compressional structures. Figure is modified from Bull et al. (2009).



$\Delta h$  (Height drop) = vertical distance between the crest of the headwall scar and the basal shear surface in the toe domain.  
 $L$  (MTD's length) = horizontal distance between the crest of the headwall scar and the farthest run out element.

## Age control

The age of the studied succession is constrained by biostratigraphic analysis of cuttings from four wells: G10-1 (interval 480-1000 m), G10-2 (480-920 m), G16-6 (600-1010 m) and M07-1 (640-760 m; Fig. 4). The Mid Miocene Unconformity (MMU) represents a hiatus that probably covers (part of) the late Middle Miocene (Serravallian) and earliest Late Miocene (earliest Tortonian), i.e. biozones DN 6-7 sensu De Verteuil & Norris (1996) and M9-11 sensu Munsterman & Brinkhuis (2004). However, as described by Köthe (2007) and Köthe et al. (2008), in well G11-1 (located very close to the study area in German waters) there is another hiatus or period of very condensed sedimentation between the early Late Miocene and the dramatic increase of the sedimentation rate which represents the onset of the delta progradation. This hiatus covers the late Tortonian - early Zanclean interval. Our age determinations show similar results, although the second hiatus seems somewhat longer. In the north-easternmost sector of the study area, wells G10-1 and G10-2 indicate a Piacenzian and 'early' Gelasian age (RT5-RT7 zones sensu De Schepper & Head, 2009) of the sequence with prograding clinoforms (Fig. 4). Aggrading reflections, representing the topset beds of the deltaic succession in the north-eastern area, have a Gelasian - Early Calabrian age (RT7 Zone sensu De Schepper & Head, 2009) and are supposed to represent the aggrading topsets in wells G10-1 and G10-2. The analysis of the post-MMU sediments in well M07-01 confirms a Gelasian age. Biostratigraphic data from well G16-6 however show a Zanclean age for the basal part of the prograding succession. The dating is based on the LOD (= Last Occurrence Datum) of dinoflagellate cyst *Reticulatosphaeridia actinocoronata*. It is possible that this taxon is reworked since seismic sections show that there are no delta lobes in G16-6 which are stratigraphically older than the ones deposited in G10-1 and G10-2 wells where we have got at least a Piacenzian age.

## Results

### The delta system

In the study area, the SNS shelf-delta represents an overall prograding system that can be recognised by a series of south-westward dipping clinoforms on top of a highly faulted Mid-Miocene Unconformity (MMU). Faults are present with a polygonal geometry at and immediately below ( $\approx 100$  ms) the surface and are interpreted as polygonal faults after Carthwright (1994). Although significant aggrading depositional phases are lacking within the clinoform succession in the study area (Fig. 2), a thick aggrading sequence overlies and truncates the prograding sequence, which is interpreted as the delta topset of coeval prograding deltaic sediment further basinward. Through time, the clinoforms tend to decrease in height, varying between roughly 500-400 m in the Piacenzian to 400-300 m in the Gelasian. The lithological variation of the prograding succession from the MMU to the top has been briefly investigated through a grain size inspection of cuttings from wells G10-1 and G10-2. Clay and silt dominate while sand is only detected in the uppermost part of the succession. Gamma-ray logs confirm the coarsening upwards trend.

In the study area, deposition onto the MMU started in the north (G quad) where the average clinoform dip indicates that the main direction of delta progradation was to the WSW, as can be seen from the projection of clinoform break point isolines (Fig. 5). This direction of progradation continues throughout depositional sequence 5. Instead, depositional sequence 6 shows a larger and better preserved delta lobe with clear lateral changes in the progradation direction (Fig. 5). In the southern sector (M quad), a SSW clinoform dip direction is visible with widely spaced clinoform breaks. To the north the progradation direction gradually changed towards the WSW and clinoform break points are more closely spaced.

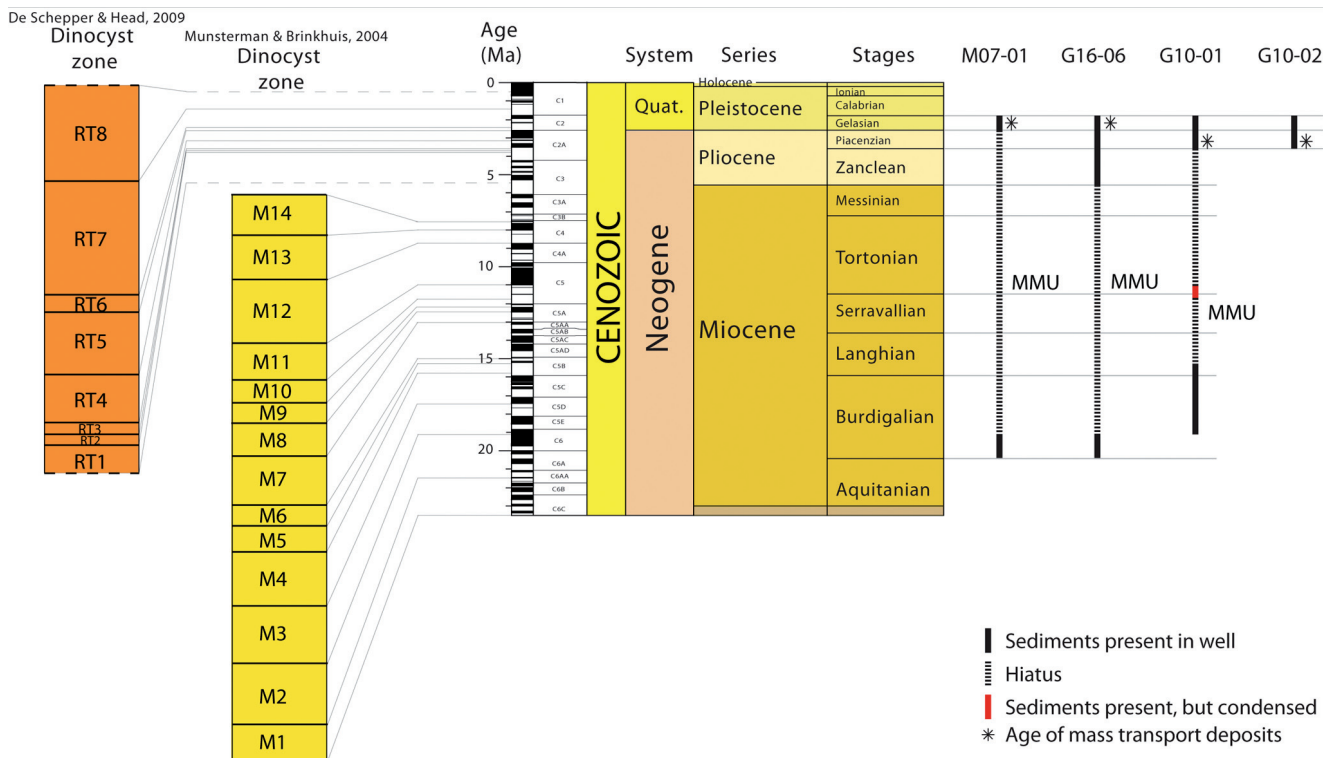


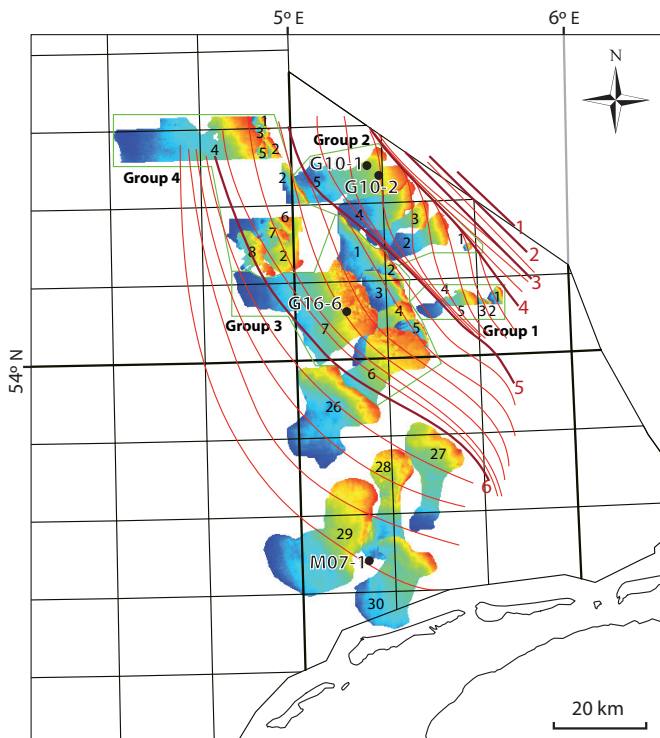
Fig. 4. Biostratigraphy of wells G10-01, G10-02, G16-06 and M07-01 based on dinocysts analysis. The hiatuses and condensed sections represent the MMU, indicating that the delta deposits and associated MTDs are of Piacenzian to (early) Gelasian age. The Zanclean age of the basal deposits directly overlying the MMU in well G16-06 are probably due to contamination since biostratigraphic analysis have been done on well cuttings (see text for further discussion). The ages of MTDs in the vicinity of the wells suggest that slope failure events become younger toward the SW, i.e. in agreement with the general direction of delta progradation.

The predominantly aggradational clinoforms in the NE-most part of the study area belong to the oldest depositional phase (Unit 1, Fig. 2). This unit is represented by depositional sequence 1-2 and the aggrading part of the depositional sequence 3. These clinoforms are rather straight in a map view (Fig. 5) and are associated with an alternation between LSTs, HSTs and, probably, thin TSTs. Overlying clinoforms turn into a more lobate shape and show a much stronger progradational character. This type of clinoform dominates most of the study area (Unit 2, Fig. 5) and is interpreted as Falling Stage System Tract (FSST) since topsets are poorly preserved and the clinoform break point position progressively falls or remains at a constant level. This succession of highly prograding sediment bodies of Unit 2 is subdivided into three different depositional sequences (final part of depositional sequence 3, depositional sequence 4 and 5) of which the areal extent progressively increases through time (Fig. 5). The first two sequences occur in the northern sector and show a small depocentre while the third one extends to the southern sector too. The clinoforms of the first two depositional sequences of Unit 2 are often marked by channel-like incisions. These erosional features mainly affect the steepest dipping sector of the slope and the area immediately basinward. A final depositional unit (Unit 3) is present in the southern sector of the study area and shows steep SSW dipping clinoforms that, towards the northwest, merge with more aggrading packages of

sediment dipping to WSW (Figs 2 and 5). Depositional sequence in Unit 3 is thus characterised by laterally changing A'/S' ratios.

MTDs are preferentially embedded in packages of steeply prograding clinoforms (Table 2). The location of slope failure events shows a progressive shift towards the south in time, reflecting the delta progradation during the last depositional stage mapped in our study area. Similarly, the direction of movement of each MTD is mostly coincident with clinoform dip direction from which delta progradation is inferred; MTDs usually move toward the WSW in the northern sector of the study area while they progressively turn to the SSW in the southern sector (Fig. 5). Another interesting relation between MTDs and the deltaic system is that the sediments deposited directly on top of and in the area immediately surrounding the MTDs tend to have a clearer progradational character (toplap terminations are better developed and reflectors are often steeper) compared to the area further away from the MTDs.

Salt-domes and ridges, belonging to the Zechstein Group are present in the entire study area. These structures did probably not directly influence the delta system in the N, but caused syn-sedimentary faulting and folding of the deltaic succession in the south producing local anomalies in delta lobe development. Salt-related faults in the southern sector are found very close to the headwall scars of some MTDs. In the northern sector however, 50 to 100 m thick mounds occur on top of the



MTD (colours identify the depth of MTD's top: red = shallow; blue = deep)  
 Trend of delta progradation within single depositional sequences  
 Initial offlap break of depositional sequence

Fig. 5. Map showing the distribution of the mapped MTDs in relation to delta progradation as depicted with clinof orm break lines. Depositional sequences 1-2 and first part of depositional sequence 3 have straight delta fronts indicative of predominantly aggrading sediments. The strongly progradational clinof orms are represented by lobate delta fronts of which the dip direction is more variable (last part of depositional sequence 3, depositional sequence 4-5-6 in the southern sector). MTDs are numbered according to their relative chronology and the group of which they are part.

MMU directly above deeper salt ridges (Fig. 6). Crestal (growth) faults rooted in the salt structure connect the mounds with the salt ridges. Moreover, sediments below the MMU, which generally only show polygonal faulting, are much more faulted under the mounds than further away. The mounds show reflectors which appear in seismic sections to be convex and to terminate onto the MMU with a downlap geometry. Most of the headwall scars in the northwest are located just above a mound ridge and follow its orientation. The sediments composing the mounds seem to be unrelated to the larger scale clinof orm progradation, but can probably be interpreted as remobilised sand from below. The remobilised Paleocene sands in the Outer Moray Firth described by Huuse et al. (2005) might be a similar kind of deposit. They suggested a model in which a phase of pervasive polygonal faulting of the overlying Paleocene and lower Eocene muds precedes the stage of fluid/sediment expulsion at the seafloor in Middle Eocene times (the Middle Eocene Unconformity).

### Location and characteristics of MTDs

In total 30 MTDs have been mapped and analysed in this study. Additional MTDs have been found at the western boundary of the study area, but have not been studied in detail. Areas and volumes of the remoulded sediment are shown in Table 3 for those MTDs where calculation of these parameters was possible.

The studied MTDs almost cover the entire study area (Figs 1 and 5), showing groups of strongly overlapping MTDs in the northern sector and a more widespread distribution in the south. Four groups (Group 1-4) including 25 MTDs have been recognised while the other five MTDs are more isolated (Fig. 5). Each group of MTDs is characterised by: 1) basal shear surfaces that tend to merge basinward; 2) occurrence in one clinof orm

Table 2. Synthesis and main characteristics of the deltaic succession and chronology of MTDs based on well-control in the vicinity of the cross-section presented in Fig. 3. Between the MMU and the aggrading post-deltaic succession the evolution of the shelf delta system is described by the shelf break (offlap break) trajectory and the inferred ratio between accommodation and sediment supply ( $A'/S'$ ; explained in Fig. 15). Note that the occurrence of slope failure events is mainly during approximate  $A'/S' \leq 0$  conditions.

Units	Depositional sequences	System tracts	Chronological control	Shelf break evolution	$A'/S'$	Group of slope failures
Post deltaic aggrading reflectors			Base is not younger than Early Calabrian			
Unit 3	Sequence 6	Transgressive - High stand	NO time control	A-P	$\approx 1$ North $0 < x \leq 1$ South	MTD 30 - MTD29 - MTD28 - MTD27 - MTD26 + not mapped more chaotic deposits in the southwesternmost sector
	Unit 2	Sequence 5		Falling stage	P-D	$\approx 0$
Sequence 4		Transgressive - High stand	Early Gelasian	A-P	$\geq 1$	GROUP 2 GROUP 1
		Falling stage		P-D	$\leq 0$	
Unit 1		Sequence 3	Transgressive - High stand	Piacenzian	A-P	$0 < x \leq 1$
	Transgressive		R		$\geq 1$	
	Low stand		A-P		$\approx 1$	
	Sequence 2	Transgressive - High stand	A-P		$\approx 1$	
		Low stand				
	Sequence 1	High stand	NO time control		A-P	$\approx 1$
	Transgressive					
	Low stand					

set; 3) a small amount of sediment deposited between different slope failure events in a relatively limited amount of time; and 4) at least partially overlapping MTDs. Within the groups, the scars of younger MTDs usually cut through older MTDs of which the headwall scar is located in a more upslope position (Fig. 7).

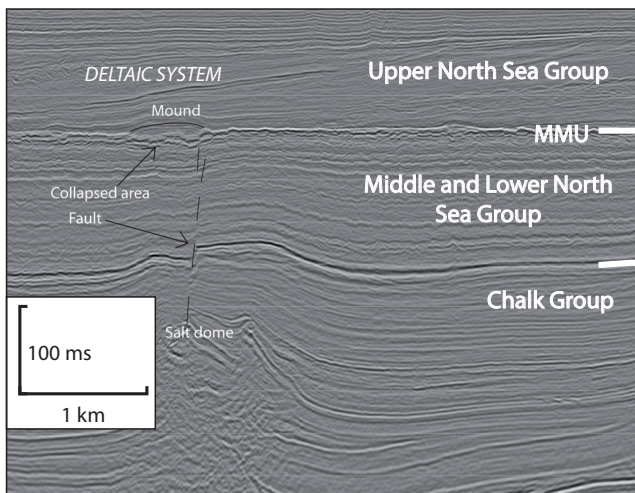
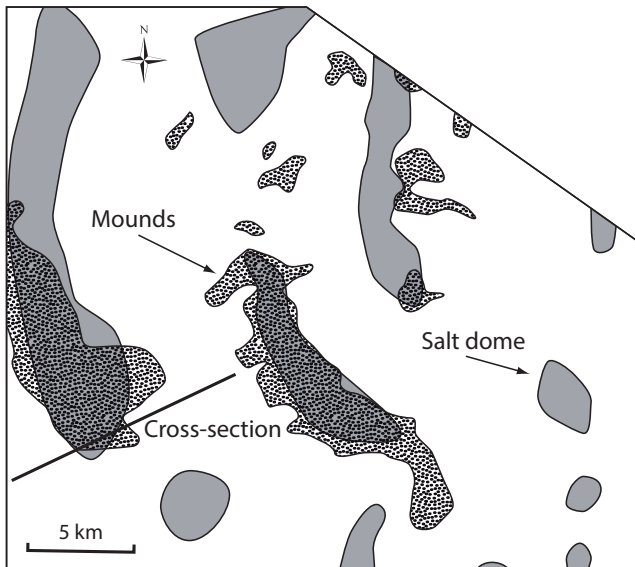


Fig. 6. Mounds on the MMU are present in the northern sector of the study area. The mounds line up with underlying Zechstein salt ridges. On seismic sections, mounds are the expression of convex reflectors downlapping onto the MMU in a limited area (usually elongated following the orientation of salt domes). The MMU seems to be collapsed in the areas of the mounds and it shows a higher than normal degree of polygonal faulting. The seismic section nicely illustrates the relation between mounds and salt ridges. Deep faults linking the two structures are clearly visible. The origin of the mounds is still unknown but it is interesting to note that the headwall scar of MTD 4-2 is located in juxtaposition with the mound and follows the same orientation. It might be possible that sediment-laden fluids ejected by salt domes created the mounds. Subsequent flows could have been released by the mounds through the overlying sediment, thereby increasing the pore water pressure. See Fig. 1 for location.

Table 3. Quantitative data for MTDs (volumes and areas). Data are not or only partially provided where calculations were not possible due to lack of seismic data or where multiple MTDs cross-cut.

Name	Area (km <sup>2</sup> )	Volume (km <sup>3</sup> )	Name	Area (km <sup>2</sup> )	Volume (km <sup>3</sup> )
MTD 1-1	-	-	MTD 3-6	265.2	27.3
MTD 1-2	-	-	MTD 3-7	426.9	41.7
MTD 1-3	-	-	MTD 4-1	-	-
MTD 1-4	-	-	MTD 4-2	-	-
MTD 1-5	>40.6	>2.9	MTD 4-3	-	-
MTD 2-1	2.8	0.1	MTD 4-4	>298.6	>33.1
MTD 2-2	97.7	4.5	MTD 4-5	>10.8	>0.5
MTD 2-3	79.3	4	MTD 4-6	17.2	1.1
MTD 2-4	>138.9	>9.8	MTD 4-7	24.3	1.5
MTD 2-5	>230.3	>17.4	MTD 4-8	50.8	27.3
MTD 3-1	-	-	MTD 26	225	27
MTD 3-2	-	-	MTD 27	180	29
MTD 3-3	-	-	MTD 28	190	28
MTD 3-4	>71	>9	MTD 29	410	46
MTD 3-5	-	-	MTD 30	230	17

### Internal geometries and shape of the MTDs

In map view, MTDs tend to be lobate with their central part (between the headwall and toe region) being most confined in width (Fig. 8). No completely depleted areas above the basal shear surface are present. The thickness of the MTDs generally decreases from the headwall domain toward the basin, following the 'pinch out' geometry of the clinoforms (Fig. 8). However, a slightly higher thickness with respect to the surrounding unfailed sediments is generally observed in the toe region.

The individual blocks of the MTDs are relatively coherent, which allows the recognition of the original internal geometry of the clinoforms. Deformation is mainly dominated by faults and fractures. Clear presence of flows or more fluidal geometries within or around the MTDs have not been found. The only exception is the ungrouped MTD deposits located in the westernmost part of the study area (F15 and F18 blocks) which have not been mapped and studied in detail.

### Basal shear surface

The studied MTDs are usually delimited by a clearly defined base. This basal shear surface represents the plane along which the material slid into the basin and which separated the MTD from the underlying sediment. In the headwall domain this surface is often represented as a strongly inclined surface ( $\approx 41^\circ$ ) cutting up through the strata (Headwall scar, Fig. 3). Along and downward this surface tilted blocks were displaced, causing a typical basin and range morphology (Fig. 9). In very few cases the basal shear surface shows a vertical offset associated with

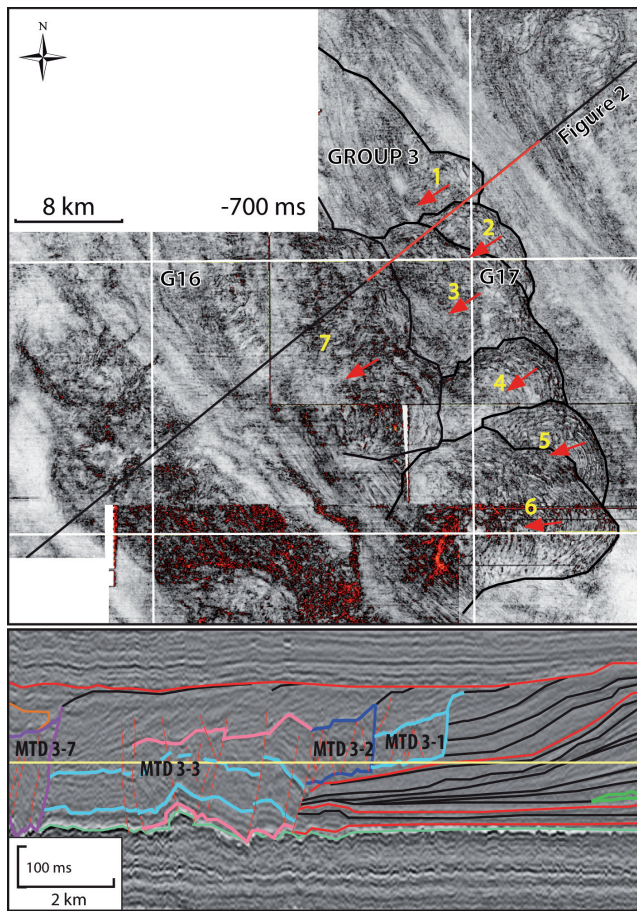


Fig. 7. Top: Time slice showing the seismic variance (coherency) attribute at  $-700$  ms TWT (see Fig. 1 for location). Seven different MTDs of Group 3 and their cross-cutting relationships are clearly visible by delineation of the MTDs in the headwall domain. In the toe domains, individual MTDs are less clearly discernable. The direction of mass movements (red arrows) is evident from kinematic indicators like rotated blocks and extensional ridges. The chronology of mass movements (yellow numbers) suggests a southward direction of propagation of slope failure events that is partly concurrent with the direction of delta progradation. Bottom: Seismic section through the stacked MTDs showing how both slope failure deposits and overlying 'higher-than-normal' prograding deposits are present in a successive MTD (see text for explanation).

extensional ramps. The basal shear surface often corresponds with the base of a clinoform or, within more aggrading sediment packages, can be associated with short transgressive phases. Generally, the dip angle of the basal shear surface decreases from the headwall domain ( $\approx 1.5^\circ$ ) to the toe domain ( $0.3^\circ$ - $0.6^\circ$ ) of the MTDs, following the general clinoform geometry.

#### MTD's top

In some MTDs, incisions have been observed in the headwall domain. These incisions show a well-developed dendritic pattern, which is usually located several kilometres landward of the headwall scar, thereby also affecting upper-slope unfailed

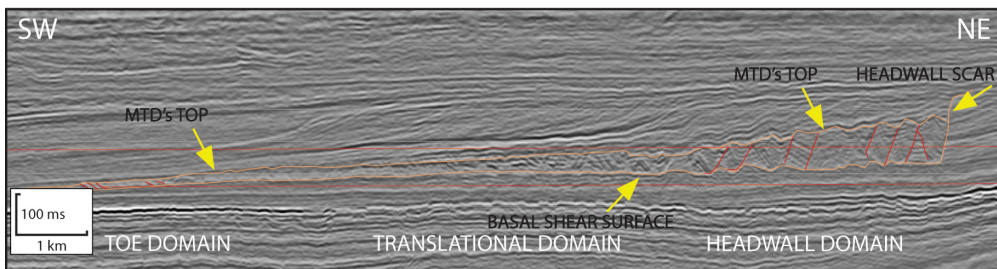
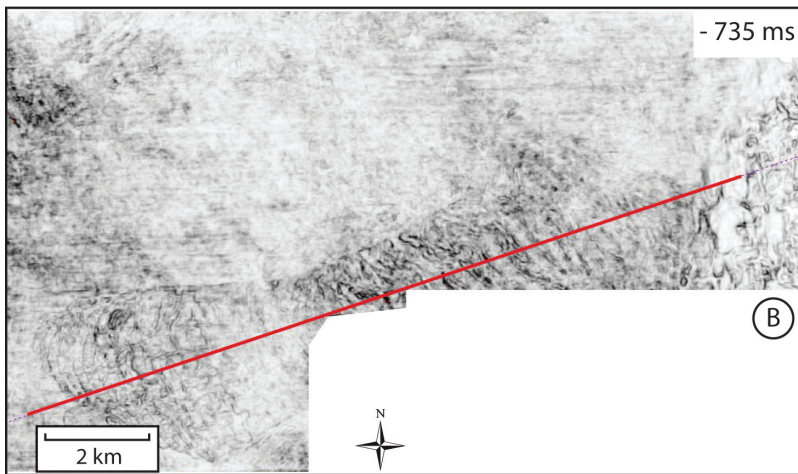
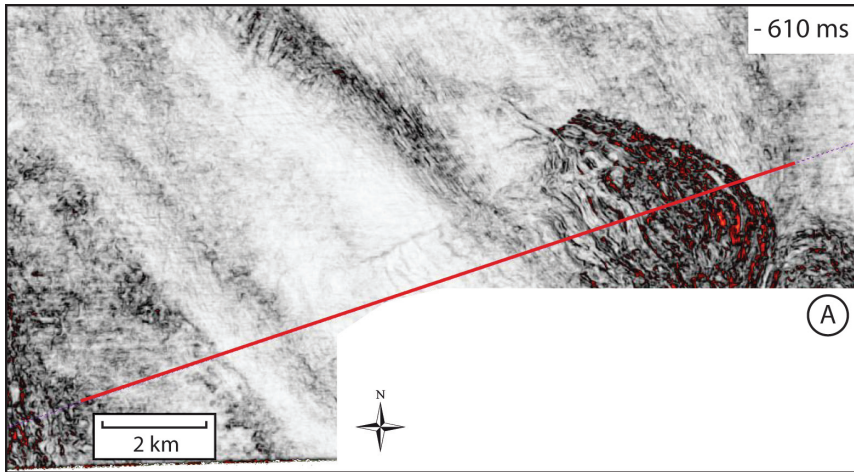
sediments. Incisions in the unfailed sediment can be very pronounced (up to 1 km wide and 60 m deep) compared to the incisions on the MTD's top (usually not more than 30 m wide and 20 m deep), suggesting that the elevation difference between the two (Fig. 10) was levelled after the slope failure event.

#### Dominant structures

The studied MTDs often show rotated blocks and extensional ridges in their headwall domain. Block dimensions (height  $\times$  length) on a seismic section can be up to  $200 \times 250$  m. Most of the associated listric normal faults sole out at the basal shear surface of the MTD. The geometry of the faults can be well studied in seismic sections without vertical exaggeration (Fig. 9). Horizontally-layered post-failure deposits are visible in the hanging walls of the rotated blocks and are overlain by a subsequent set of clinoforms deposited during renewed 'normal' delta progradation. In some MTDs the tilt blocks are affected by another set of probably younger faults and fractures characterised by a more variable geometry. This faulting results in a complex framework of structures which is more characteristic for the central sector of MTDs.

The central sector of the MTDs can be both characterised by a substantial lack of structures and by a high number of faults and fractures, which complicate the recognition of the structural framework. The translational domain does not show a clear dominance of either extensional or compressional deformation. Geometries vary within the same MTD and between different ones. In some cases, pop-up like structures can be recognised (mainly in the central part of the MTDs but sometimes over the entire MTD's length; Fig. 11a). These are bounded by two sets of faults with an opposite dip direction that cause the top of the MTDs to be folded into anticlines and synclines with an orientation perpendicular to the direction of mass movement. These pop-up geometries result in a ridge and basin topography, similar to the geometry resulting from the rotated blocks in the headwall domain. In a few cases bright spots (Fig. 11a) are found in anticlines directly on top of the MTD, suggesting trapping of gas occurred in the non-faulted overburden.

The thickness of the MTDs generally decreases toward the basin and becomes close to or below the resolution value of the seismic data in the toe region. Individual reflectors in the toe domain are therefore not easy to recognise; the seismic facies tend to be chaotic. The chaotic appearance might be an artefact related to lack of resolution. Where it is possible to distinguish features, thrusts and blind thrusts are the most common structures that can be found in the lowermost sector of the MTDs (Fig. 11b).



— fault  
— top and base of MTD

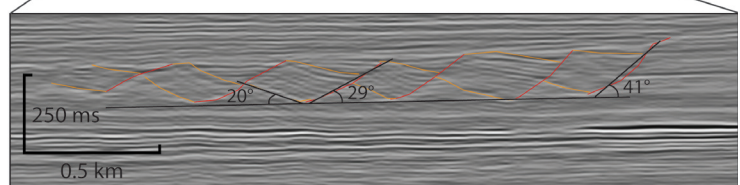
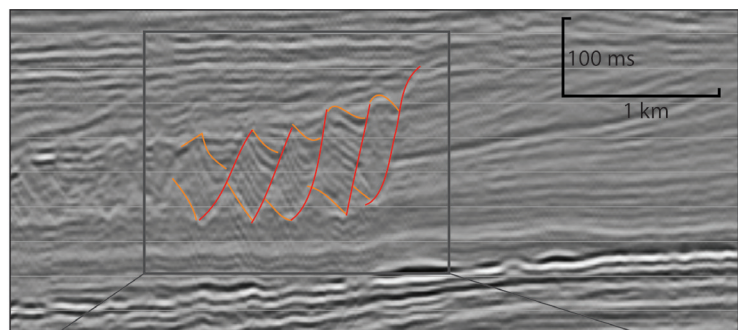


Fig. 8. (Top) Two time slices showing the seismic variance (coherency) attribute at  $-610$  ms (A) and  $-735$  ms (B; see Fig. 1 for location). MTD 1-5 is shown here; rotated blocks and extensional ridges are particularly well visible in A while thrusts and pressure ridges can be seen in B. (Bottom) Seismic section through MTD 1-5 showing the coherent aspect of the internal reflectors. The profile of the MTD shows a decreasing thickness toward the basin, in agreement with the typical shape of clinoforms involved in the failure. The remoulded mass is mainly maintained close to the headwall scar. These characteristics, together with the lack of completely depleted areas above the basal shear surface, suggest a dominant brittle deformation and a minor mass displacement. Therefore, it is supposed that mass movement ceased soon after the slope failure. These are the typical characteristics of the MTDs in the study area.

Fig. 9. Rotated blocks in the headwall domain of MTD 1-5. The same seismic section is shown with 5x of vertical exaggeration (Top) and with no vertical exaggeration (Bottom) (see Fig. 1 for location). The blocks are well visible in both sections. The dip value of the headwall scar, the listric faults bounding the blocks and the base of the rotated blocks are shown. Post failure sediment deposited on top of the MTD is visible between the rotated blocks. The horizontal layering of these reflectors suggests that the process of block rotation ceased before sediment deposition reprised after the failure event.

## Discussion

### Delta evolution

The most important characteristics of the SNS shelf-delta system in the study area are: 1) a comparable size to the greatest actual deltaic systems (i.e.: Niger Delta); 2) a decrease in clinoform height through time; 3) a predominance of depositional phases characterised by a constant or even a decrease in accommodation space (well visible from the onset of Unit 2); and 4) the general lack of preserved transgressive sequences even during periods of rising sea-level (Fig. 2). The consistency between biostratigraphic analysis and palaeobathymetric reconstruction from clinoforms thickness in the Southern North Sea (Cameron et al., 1993; Laursen et al., 1997; Huuse, 2002) suggests the interpretation of a progressive sea level lowering from the onset of Unit 2. A sea-level fall is also in agreement with Sørensen et al. (1997) who suggested that the sediments of their composite sequences VI and VII (Fig. 12) were deposited during a sea-level fall while the preceding and successive composite depositional phases were not. The sea-level lowering is probably reflected in the more limited areal distribution of the sediments belonging to sequence VI and VII (equivalent to the succession studied here) compared with the other composite sequences (Fig. 12). On the time scale considered, the regional tectonic subsidence likely was a linear process, whereas glacio-eustatic variations showed higher-frequency variations with amplitudes up to 100 m in the Gelasian period (Miller et al., 2005). Plio-Pleistocene accelerated subsidence in the North Sea Basin due to sediment load (Van Wees & Cloetingh, 1996) was temporarily outpaced by decreasing water depths caused by intensification of Northern

hemisphere glaciations, which explains both variations in eustasy and sediment supply. Overall, a glacio-eustatic fall may be the reason why topsets of Units 2 and 3 are not well preserved in the study area. The aggrading sediment package on top of the prograding succession forms the topsets to foresets deposited further WSW of the current study area (probably represented by the composite sequence VIII of Sørensen et al., 1997). The shallow marine topsets are clearly deposited under the influence of (full) glacial climatic conditions as is attested by the numerous iceberg scour marks (Kuhlman & Wong, 2008).

The prograding wedges east of our study area in German waters have been dated Zanclean and Piacenzian (Köthe, 2007; Köthe et al., 2008). Based on biostratigraphic analysis of the wells shown in Fig. 1, the age of the delta sediments deposited in our study area ranges from Piacenzian to Gelasian, which is in accordance with the results obtained in the German sector and the delta progradation direction. However, Sørensen et al. (1997) proposed a Zanclean and Piacenzian age for the same succession. Sørensen et al. (1997) based their interpretation merely on stratal relations rather than biostratigraphic data, so we give priority to our age determinations. In addition, Kuhlman & Wong (2008) proposed younger ages for the older prograding sediment in the northern sector of the Dutch SNS than the one Sørensen et al. (1997) suggested. Apart from the difference in age interpretations, the results of our study fit very well in the overall reconstruction presented by Sørensen et al. (1997). The ages of the falling stage sediments agree well with the eustatic and  $\delta^{18}\text{O}$  curves from Miller et al. (2005), who show a climatic cooling during late Piacenzian and Gelasian times related to increased Northern hemisphere glaciation.

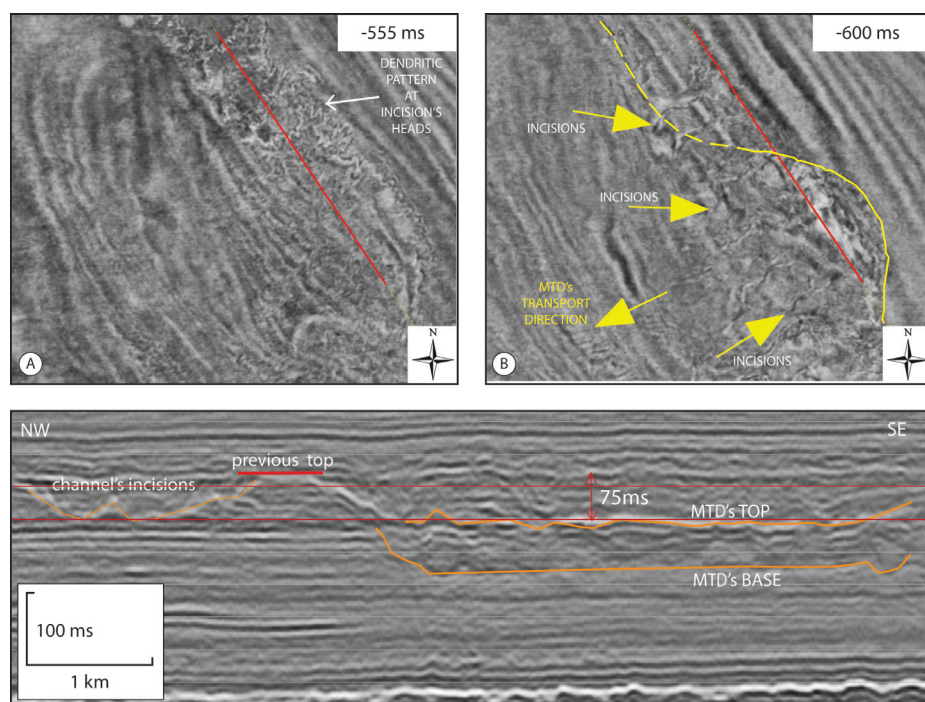
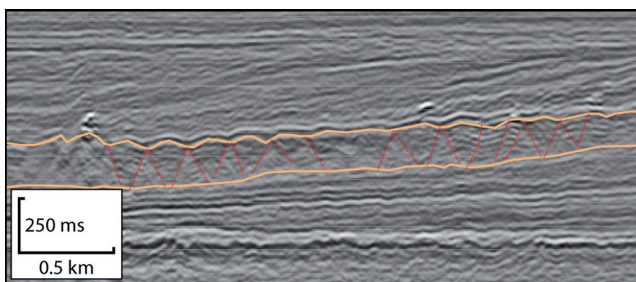
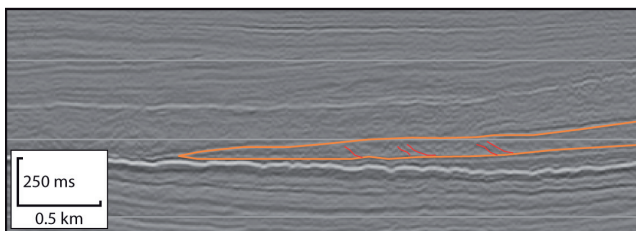


Fig. 10. (Top) Two time slices at different TWTs (-555 ms (A) and -600 ms (B)) showing channels on top of MTD 3-1 (see Fig. 1 for location). Channels show a sinuous shape and a well visible dendritic pattern at their heads. These affect the headwall domain of the MTD whereas they disappear towards the basin. Moreover, they are also visible on unfailed sediment upslope the headwall scar. (Base) Seismic section oriented perpendicularly to MTD 3-1 showing that channels are much more visible on unfailed sediment than on top of the MTD. A drop of 75 ms (roughly 75 m) between the palaeo sea-floor and the new MTD's top is visible on the left side of the seismic section. This drop explains the stronger erosion of the sediment upslope the headwall scar than on top of the MTD.

Overall, delta progradation rates (to the WSW) in the study area were initially the highest in the northern part of the study area. Through lobe switching, sedimentation supply and progradation also gradually increased in the south, as reflected by the changing direction of progradation from predominantly WSW to SSW between Units 2 and 3. After complete infill of the northern part of the study area, accommodation had diminished and the delta system was forced to migrate further to the south. For Unit 3 it can be inferred that simultaneous with rapid progradation in the south, aggradation took place in the north (Fig. 5). Possibly, the presence of salt domes in the southern and southeastern part of the study area might have forced the Unit 1 and 2 sediments northward due to a slight positive relief on the palaeo-coastal plain. A falling sea-level could have enlarged the effect of salt-dome topography on steering the direction of delta progradation. It is thus suggested that glacio-eustasy is the dominant control on the evolution of the studied delta system whereas subsidence controlled accommodation on a regional scale. Salt tectonics may have induced lobe switching on a more local scale, although autogenic processes cannot be ruled out.



a.



b.

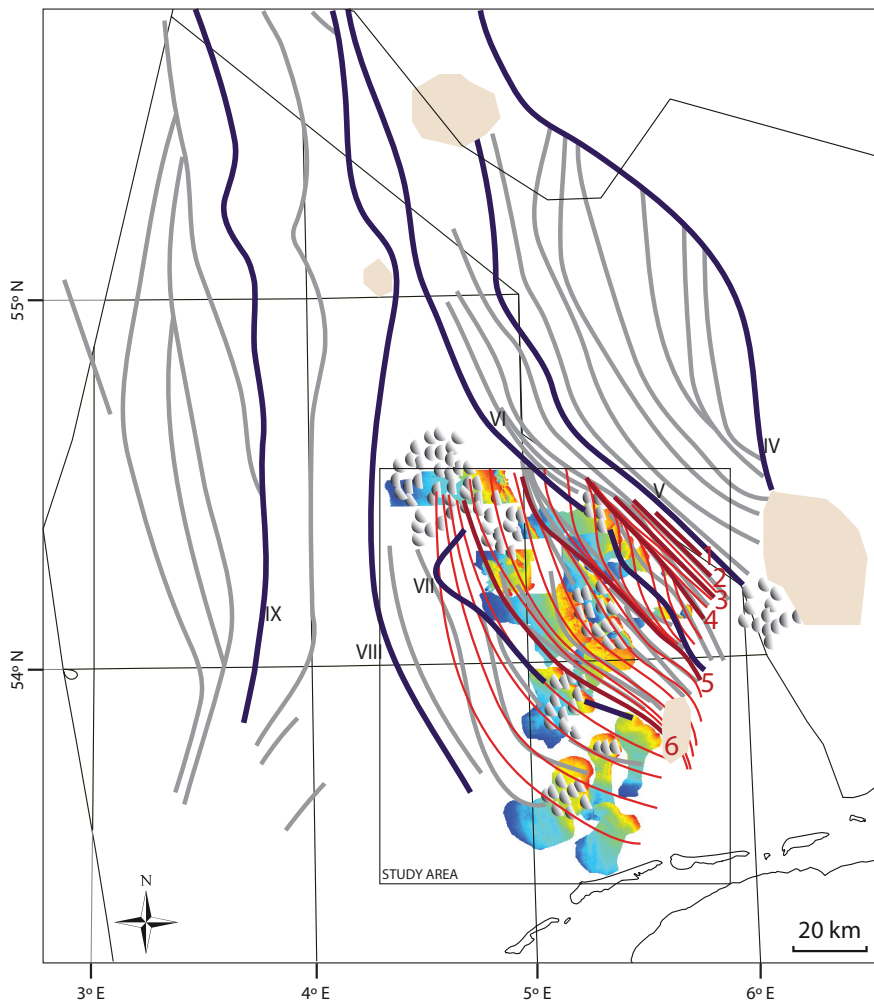
Fig. 11. a. Pop-up structures in the updip sector of the accumulation zone are visible in a seismic section through MTD 2-5 (see Fig. 1 for location). The section shows well visible internal reflectors and two main families of faults causing positive relief on the MTD's top. The sediment deposited after the mass movement took place also shows a curvy aspect in correspondence with the anticlines. A change from extensional to compressive deformation after the mass movement ceased is somehow required to explain the presence of these structures close to the headwall scar. b. Seismic section showing compressive structures in the toe region of MTD 3-7 (see Fig. 1 for location). Thrusts and blind thrusts are the dominant structures in the accumulation area according to literature. However, they are often difficult to identify since the vertical thickness of the MTD's toe domain is usually close to the seismic resolution.

## MTDs evolution

The limited amount of sediment removal from the headwall domain (lack of completely depleted areas above the basal shear surface), the lack of an emergent toe lobe on top of unfailed sediment in the toe-domain, the strong coherence of the failed material and the dominance of brittle deformation suggest that mass movement usually ceased relatively soon after the slope failed. Due to the development of normal faults, pore water pressures in the basal shear surface are expected to rapidly decrease (Micallef et al., 2007), thus increasing the shear strength (Fig. 13). In addition, a low and decreasing dip angle of the slope toward the downslope area might also have prevented the mass transport to accelerate (c.f. Huvenne et al., 2002). Therefore, the geometry of the MTDs in the study area reflects to a large extent the original shape of the failed sediment package. The MTDs pinch out not far from where their correlative clinofolds pinch out.

The basal shear surface is usually located at the base of a prograding clinofold or within a thin aggrading package of sediment at the basin floor. These sediments are supposed to be usually associated with a higher clay content since they were deposited during phases in which the sedimentation rate (especially the coarser input) was relatively low (i.e. when clinofolds were not formed). Clay content may therefore play a role in determining the position of the basal shear surface; high pore water pressures are more likely to develop in layers with lower permeability (Popenoe et al., 1993; Hampton et al., 1996; Locat & Lee, 2002; Canals et al., 2004; Masson et al., 2005; Owen et al., 2007; Lee, 2009; Fig. 13).

Frey-Martinez et al. (2006) distinguish between two end-members of submarine landslides; frontally confined and frontally emergent. The final geometry of a submarine landslide depends on the ability of the moving mass to ramp up from its basal shear surface and subsequently translate in an unconfined way over the seafloor (frontally emergent). The thickness of the moving material and thus the depth of the basal shear surface is the key factor that regulates the behaviour of the mass movement. If the thickness of the mass movement is too large, the energy needed to ramp up the basal shear surface is likely to be insufficient which causes the mass movement to remain confined. In cases of a rather shallow basal shear surface (tens of meters) the mass movement will have a higher chance of overflowing the (undeformed) material in the downslope region. However, in our study area the basal shear surface is relatively shallow (such that the mass movement will have a higher chance of overflowing the (undeformed) material in the downslope region), but an evident ramp was not developed, nor clear indications of overflowing sediments. Sediments confining the mass movement are not present either; the shape of the MTDs is related to the pinch-out shape of prograding clinofolds (Figs 8 and 11b). Altogether, due to the lack of both thick unfailed sediments constraining the



**Interpretation Sorensen et al. (1997)**

- Slump
- Offlap Break of individual sequences
- Initial offlap break of composite sequence
- Salt disturbance

**This study**

- MTD (colours identify the depth of MTD's top: red = shallow; blue = deep)
- Trend of delta progradation within single depositional sequences
- Initial offlap break of depositional sequence

Fig. 12. Comparison between this study and results of Sørensen et al. (1997). Our interpretations correspond mostly with Sørensen's composite sequences VI and VII. These were suggested to be controlled by low sea-level conditions based on reflection terminations and the lobate shape of delta fronts. This study confirms this hypothesis and proposes a progressive sea-level fall from the last part of depositional sequence 3, which approximately corresponds with the onset composite sequence VI of Sørensen et al. (1997). Despite the resolution differences, both studies confirm that MTDs are only present in the falling stage sequences and are missing in other composite sequences of which the areal extent is considerably larger.

MTDs in the toe region and ramps making the mass movement to overthrust unfailed sediment above the seafloor, the MTDs observed in this study can neither be classified as frontally confined nor as frontally emergent. Therefore, the studied MTDs should be considered a new intermediate type of submarine landslides which has not been described before. The different aspect and therefore, the different behaviour, of this new type may be associated with the combined effect of the relatively short time of actual sediment movement and the clinoform shape of the sediment constituting the slope before the failure. The relatively small transport distance (and momentum) of the failed material toward the basin is supposed to have not been able to cause the mass movement to overflow the downslope undeformed material although the limited thickness of the clinoform in the basin did not form a clear obstacle for the failed material to remain confined.

There is evidence for a change of an extensional to a compressional regime through the evolution of the single mass failure event (Fig. 13). The presence of symmetrical pop-up like structures in the central part of the MTD but very close to the headwall scar requires such a change in regime. This suggests that compressive deformation was superimposed on extensional structures at times when the mass movement

ceased: normal faults were inverted and new compressional faults developed.

Most of the MTDs are part of a clearly defined group (Fig. 5). The alternation between sediment deposition and slope failure and the observation that a successive MTD mostly occurs basinward of the previous one shows that there is a progressive rather than a retrogressive evolution within the group. In a retrogressive system, successive MTDs should develop landward without intervening sediment deposition. In that case, they would be considered different parts of the same MTC (Mass Transport Complex sensu Bull et al., 2009) since they would represent the same slope failure event.

The observation of incisions in the unfailed material upslope of the headwall scars and in the MTDs top and headwall scars themselves suggests that erosive flows developed after the mass movement took place (Figs 10 & 13). The generation of erosive currents in the upper part of submarine slopes has been related to sea-level falls even when incisions do not continue landward and subaerial exposures are not visible (Overeem et al., 2001; Ethridge et al., 2005). However, when the incisions are related to sea-level fall, one would expect to find incisions in other (undisturbed, age-equivalent) parts of the delta too. Since this has not been observed, we propose

that the incisions in the MTDs are related to a concentration of the drainage (hyperconcentrated flow) across the steep relief created by the headwall scar (Fig. 13). The stronger progradational character of clinoforms on top of failed materials compared to areas further away confirms this interpretation of localised sediment supply to the delta front (Fig. 13).

### Causes for slope failure

The MTDs in our study area are exclusively associated with Unit 2 and 3, which represent deposition during progradational depositional phases (low  $A'/S' \approx 0$ ; Table 2). Unit 1, which is clearly aggrading ( $A'/S' \approx 1$ ), is the only unit where MTDs are lacking. Therefore, we propose that the combination of low accommodation space and high sediment supply was a precondition for slope instability (Fig. 14). This is in agreement with

Overeem et al. (2001) who also suggested that sea-level fall might have triggered slope failure. Moreover, deposits related to submarine landslides have been identified by Sørensen et al. (1997) within their composite sequences VI and VII (equivalent to the sediments studied here) while they are virtually missing in the other depositional sequences they mapped. The main difference between sequences VI and VII and the other units described by Sørensen et al. (1997) is that the other units are characterised by a much more extensive areal distribution along the Southern North Sea shelf delta system than the former (Fig. 12).

Based on the observation of stacked MTDs in the northern sector (Fig. 7) it is inferred that a single slope failure event might be considered a preconditioning factor for another slope failure event in settings dominated by high sediment supply and minor changes in accommodation space. A plausible mechanism is that the concentrated increase in sediment supply across

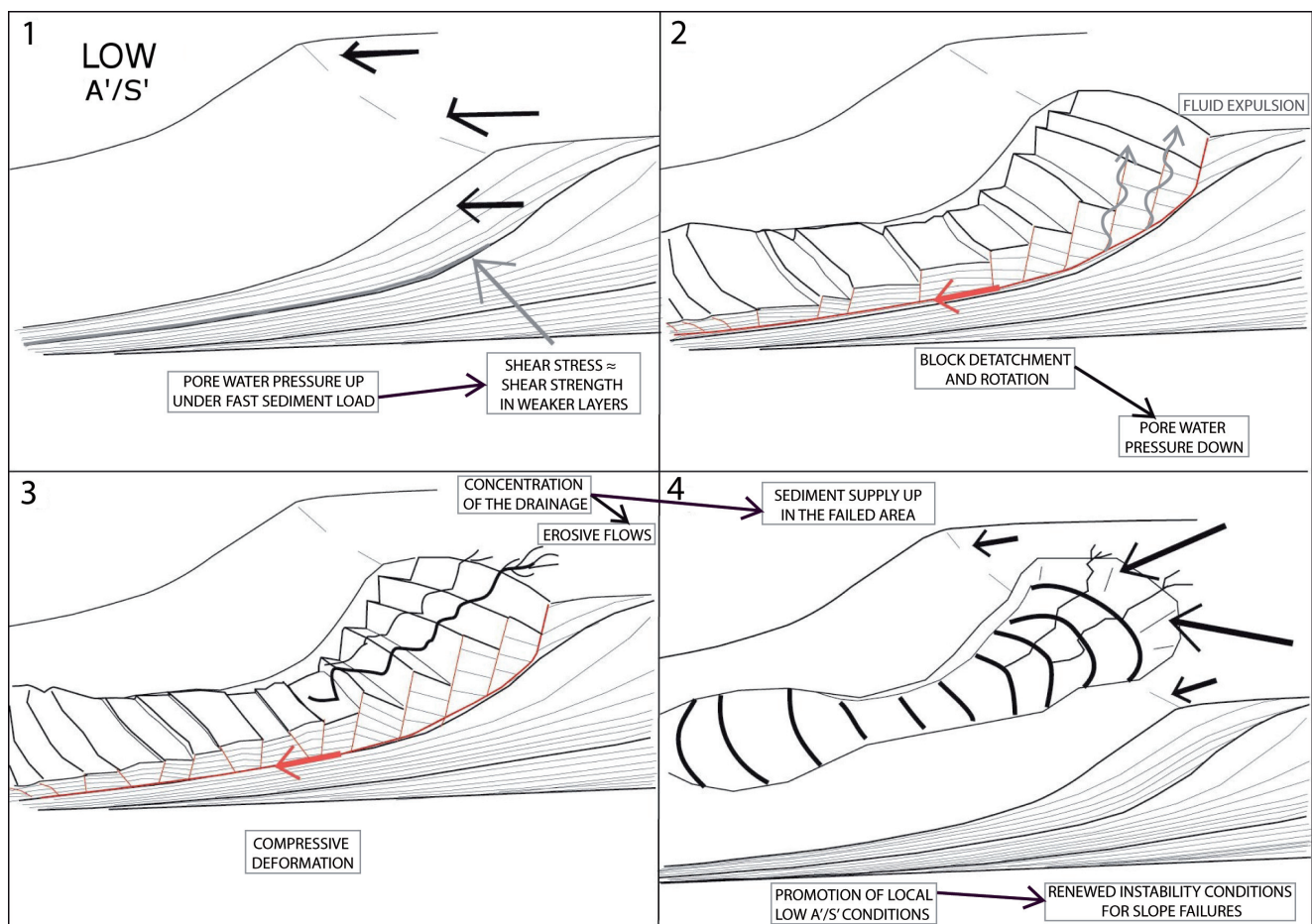


Fig. 13. Schematic representation of the typical four-stage slope failure evolution for this study. Stage 1: Initiation of mass movement along a weak layer, where the shear strength of the sediment has overcome. Stage 2: Rotating blocks and extensional ridges develop in the headwall domain while faults and fractures with a more variable dip probably develop elsewhere. Faults and fractures connect the basal shear surface with the sea floor, thereby facilitating fluids to escape and leading to decrease of pore water pressure. The subsequent increase in shear strength and the decreasing dip angle of the basal shear surface toward the basin cause the mass movement to cease soon after slope failure initiation. Stage 3: Once the mass movement stopped, drainage focuses in the negative relief of the headwall domain causes incisions. Stage 4: Drainage concentration in the failed area continues and promotes local higher sedimentation rates, explaining the strong progradational depositional style on top of the MTDs. This promotes renewed instability in the area where the slope already failed and the cyclic and cross-cutting formation of MTDs.

headwall scars following events of slope failure (see above) uphold the low  $A'/S'$  conditions and favour a continuation of the instable slope conditions (c.f. Masson et al., 2005). Subsequently, a new MTD develops after which the sediment delivery through incised valleys is localised again. Since the head scars of younger MTDs usually cut through older MTDs and are positioned in a more basinward position, it is suggested that the stacked MTDs represent continuous diminishing of accommodation and are part of the same FSST. As such, the conditions for slope failure exist as long as the low  $A'/S'$  conditions pertain (Fig. 14).

It is suggested that a specific slope-failure trigger is required in order to overcome the shear strength of the sediment (Popenoe et al., 1993; Mc Gregor et al., 1993; Hampton et al., 1996; Locat & Lee, 2002; Canals et al., 2004; Owen et al., 2007; Masson et al., 2005; Lee, 2009). Seismic events are considered the most common trigger for slope failures (Hampton et al., 1996; Locat & Lee, 2002; Canals et al., 2004 and references therein; Masson et al., 2005; Owen et al., 2007; Lee, 2009). Since important faults in the study area are supposed to have been inactive from Early Cretaceous onwards (Ziegler, 1990), large-scale tectonics has not been considered an important triggering factor for the studied slope failure events. However, in the southern sector salt domes and ridges clearly influence the shelf delta system by synsedimentary faulting and folding. Since active salt doming is strongly related to regional tectonic activity (Ten Veen et al., this issue), this observation puts doubt to the notion that tectonics did not play a role. Furthermore, the presence of headwall scars in proximity to salt-related faults that affect the entire deltaic succession, for instance for MTD 27, is considered a strong indication that halokinesis may induce seismicity (Leith & Simpson, 1986) and fluid release

especially in the south of the study area. In the northern sector, where prominent salt-domes are lacking, salt-related triggering is less likely. The MTDs of Group 4 may form an exception since the main headwall scars are located exactly above mounds visible on the MMU. These mounds seem to be connected via faults to underlying salt-domes (Fig. 6). Slope failures could have been triggered in the event fluid venting occurred from these mounds, thereby decreasing the shear strength of the overlying sediments. Although this clearly needs further investigation, the relationship between the mounds, the salt walls and the location/orientation of the headwall scars of the MTDs of Group 4 suggests a possible link between these structures and the instability of the slope. In deltaic settings, locally very high sedimentation rates are supposed to be a triggering factor for slope failures too (Martinsen, 1994; Hampton et al., 1996; Masson et al., 2005, Leynaud et al., 2009). However, the lack of sedimentation rate figures does not permit us to draw conclusions on this matter. Another possible trigger for delta settings is the cyclic loading by storm waves (McGregor et al., 1993; Hampton et al., 1996; Locat & Lee, 2002; Owen et al., 2007). Huge storm-related waves can create seismicity in shallow waters down to approximately 100 m deep (Hampton et al., 1996). Since the headwall scars of the mapped MTDs are always located close to the clinoform break point and so to shallow water domains, it is possible that the sedimentary succession was affected by the effect of wave loading due to storms. Moreover, high frequency sea-level falls (suggested by incisions on the slopes within FSSTs) and a general trend in decreasing sea level in the whole deltaic succession could have made the steep coastline more vulnerable to the effect of storm waves' loading. Slope oversteepening, sometimes suggested as a triggering factor for mass movements in deltaic environments

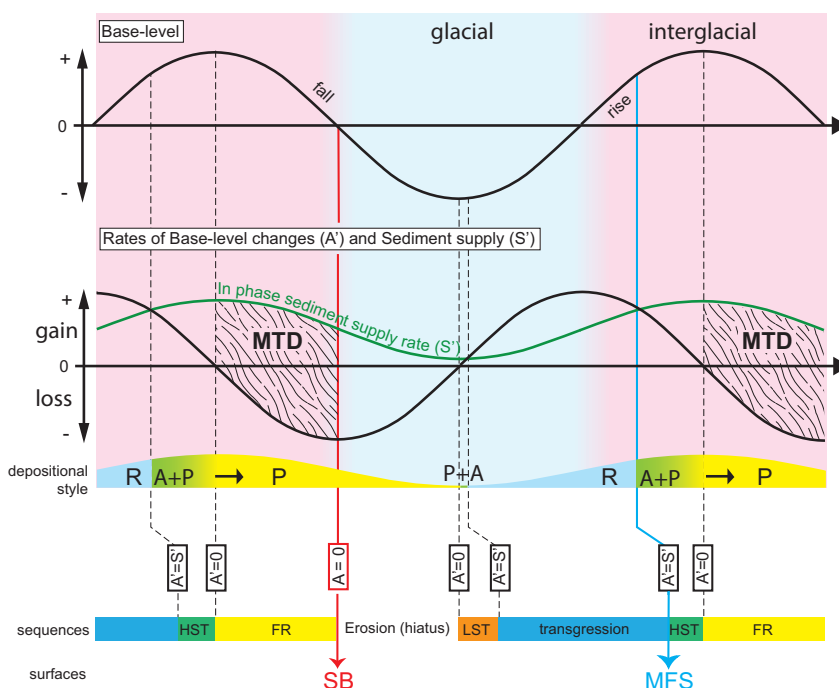


Fig. 14. Conceptual model explaining the relationship between climatically controlled variations in sediment supply ( $S'$ ) and accommodation change ( $A'$ ) in a setting dominated by glacioeustasy. The periglacial setting of the Pleistocene SNS shelf-delta is best explained by an in-phase relationship, where low supply occurs at sea-level lowstand (glacials). The diagram explains that lowstand deposits (LST) are unlikely to form due to 1) limited sediment supply to the basin and 2) a short time window. Instead, highstand deposits are thick and initially aggrading (A) due to both sufficient accommodation and supply. Forced regressive wedges (FR) or FSST are strongly progradational (P) and are topped by an erosional unconformity and a phase of degradation (D) and retrogradation (R) during subsequent transgression. Higher-order sea-level trends on the falling limb may explain the stacked nature of the MTD's. Concept based on Catuneanu (2006) and Ten Veen et al. (2008).

is not considered a determinant mechanism for MTDs formation in the study area since slope failures occur in not so steep clinoforms ( $\approx 2^\circ$ ) while they miss where the steepest clinoforms are (up to  $8^\circ$ ).

In summary, we suggest that high frequency sea-level falls in combination with high sediment supply gave rise to periods of very low or even negative  $A'/S'$  ratios, which increased the slope instability and thus the probability for MTDs to develop in the study area. A possible explanation, in line with most of the previous studies mentioned herein, is that alternations of glacial/interglacial conditions during the Gelasian caused linked sea-level and sediment supply variations. Storm waves' loading and local halokinetic activity are two possible processes that might have induced local seismicity to trigger failure of the sediment filled slope.

## Conclusion

- By means of continuous progradation, the SNS shelf-delta system progressively filled the study area (G & M offshore blocks in the Netherlands) between the Piacenzian and the (early) Gelasian. This age agrees with the Zanclean-Piacenzian age of the prograding system in the German sector (Köthe, 2007 and Köthe et al., 2008) where stratigraphically older sediments are present.
- Progradation was mainly to the WSW but in the southernmost sector a counter-clockwise change toward SSW occurred over time. This change in the south might have been caused by the presence of active salt domes and ridges that formed obstructions to delta progradation in the early phase.
- Reflector geometries analysed on both seismic sections and time slices show lobate prograding clinoforms with vertical thicknesses decreasing with time. This suggest that sediment supply has been high for the entire studied succession and that there was a progressive lack of accommodation creation ( $A'/S' \leq 0$ ). This is agreement with Sørensen et al. (1997) who suggested a progressive sea-level fall during composite sequences VI and VII (in their work) which are located in the present study area.
- The delta front failed several times, creating at least 30 internally coherent mass transport deposits (MTDs), which are grouped according the clinoform set that is affected. MTDs in the same group often partly overlap and share a basal shear plane. Five MTDs in the southern part of the study area are more randomly distributed and are not part of a group.
- The most important features of the studied MTDs are: 1) the dominance of brittle deformation; 2) small amount of material removal from the headwall domain (lack of completely depleted areas on top of the basal shear surface); and 3) the lack of an emergent toe domain above the un-failed sediment located basinward although proper confining geometries are not detected. Therefore, the studied MTDs

can neither be classified as frontally confined nor as frontally emergent but they are a new intermediate type of submarine landslides which has not been described before. Mass movement is supposed to have ceased relatively soon after initiation of failure. The last phase of movement has predominantly been compressive since pop-up structures have been observed in places of initial extensional deformation.

- The chronology and direction of movement of the MTDs reflect the direction of delta progradation as represented by westward inclined clinoform sets that become younger toward the southwest.
- The incisions on the top of MTDs suggest the presence of erosive flows. These flows were probably generated due to a concentration of the drainage caused by the negative morphology the failure event left behind on the upper sector of the slope. The higher prograding character of the reflectors on top of MTDs suggests that concentration of drainage continued after the erosional phase.
- The main precondition for slope instability is thought to be the interplay between high sediment supply and constant or even decreasing accommodation space (caused by glacio-eustatic sea-level fall). The general lack of MTDs embedded in more aggrading phases of the Neogene-Quaternary SNS shelf-delta system (Sørensen et al., 1997) is in line with this. In addition, local high sedimentation rates in areas of a recent slope failure are supposed to have been another important factor for slope instability. The presence of groups of stacked MTDs and the higher prograding aspect of sediments on top of MTDs confirm this hypothesis and suggest that slope failures could also be considered a preconditioning factor in settings dominated by high sediment supply.
- In places where salt domes are found, salt-induced seismicity and upward fluid escape are considered important triggers for slope failure. Other mechanisms such as storm wave loading on exposed delta slopes might be plausible as well.

## Acknowledgements

The authors would like to thank Mads Huuse and Mark Geluk for their thorough review of the manuscript and the constructive comments provided. The idea of the research behind this paper was launched when Ed Duin (TNO) addressed the chaotic features in the seismic data he was interpreting at the time. Thanks to his suggestions we have been able to start a fruitful cooperation between the mapping team and geobiology at TNO, leading to this manuscript. Most of the work was done by interns (A.B. and F.B. from Florence University, Italy (see authors list)), but the paper also benefited from the work of several master students from Manchester University.

## References

- Bijlsma, S.**, 1981. Fluvial sedimentation from the Fennoscandian area into the Northwest European Basin during the Late Cenozoic. *Geologie en Mijnbouw* 60: 337-345.
- Bull, S., Cartwright, J. & Huuse, M.**, 2009. A review of kinematic indicators from mass-transport complexes using 3D seismic data. *Marine and Petroleum Geology* 26: 1132-1152.
- Cameron, T.D.J., Bulat, J. & Mesdag, C.S.**, 1993. High resolution seismic profile through a Late Cenozoic delta complex in the southern North Sea. *Marine and Petroleum Geology* 10: 591-600.
- Canals, M., Lastras, G., Urgeles, R., Casamor, J.L., Mienert, J., Cattaneo, A., De Batist, M., Hafliðason, H., Imbo, Y., Laberg, J.S., Locat, J., Long, D., Longva, O., Masson, D.G., Sultan, N., Trincardi, F. & Bryn, P.**, 2004. Slope failure dynamics and impacts from seafloor and shallow sub-seafloor geophysical data: case studies from the COSTA project. *Marine Geology* 213: 9-72.
- Cartwright, J.A.**, 1994. Episodic basin-wide fluid expulsion from geopressed shale sequences in the North Sea basin. *Geology* 10: 591-599.
- Catuneanu, O.**, 2006. *Principles of Sequence Stratigraphy*. Elsevier (Amsterdam), 375 pp.
- Catuneanu, O., Abreu, V., Bhattacharya, J.P., Blum, M.D., Dalrymple, R.W., Eriksson, P.G., Fielding, C.R., Fisher, W.L., Galloway, W.E., Gibling, M.R., Giles, K.A., Holbrook, J.M., Jordan, R., Kendall, C.G.S.C., Macurda, B., Martinsen, O.J., Miall, A.D., Neal, J.E., Nummedal, D., Pomar, L., Posamentier, H.W., Pratt, B.R., Sarg, J.F., Shanley, K.W., Steel, R.J., Strasser, A., Tucker, M.E. & Winker, C.**, 2009. Towards the standardization of sequence stratigraphy. *Earth Science Reviews* 92: 1-33.
- De Jager, J.**, 2003. Inverted basins in the Netherlands, similarities and differences. *Netherlands Journal of Geosciences* 82: 355-366.
- De Lugt, I.R.**, 2007. Stratigraphical and structural setting of the Palaeogene siliciclastic sediments in the Dutch part of the North Sea Basin. PhD thesis, Utrecht University (Utrecht), 112 pp.
- De Schepper, S. & Head, M.J.**, 2009. Pliocene and Pleistocene dinoflagellate cyst and acritarch zonation of DSDP hole 610a, Eastern North Atlantic. *Palaeogeography, Palaeoclimatology, Palaeoecology* 33: 179-218.
- De Verteuil, L. & Norris, G.**, 1996. Miocene dinoflagellate stratigraphy and systematics of Maryland and Virginia. *Micropaleontology* 42: 1-172.
- Eidvin, T., Riis, F. & Ruundberg, Y.**, 1999. Upper Cainozoic stratigraphy in the central North Sea (Ekofisk and Sleipner fields). *Norsk Geologisk Tidsskrift* 79: 97-128.
- Ethridge, F.G., Germanoski, D., Schumm, S.A. & Wood, L.J.**, 2005. The morphologic and stratigraphic effects of base-level change: a review of experimental studies. In: Blum, M.D., Mariott, S.B. & Leclair, S.F. (eds): *Fluvial Sedimentology VII*. International Association of Sedimentologists, Special Publication 35: 213-241.
- Frey-Martinez, J., Cartwright, J. & James, D.**, 2006. Frontally confined versus frontally emergent submarine landslides: A 3D seismic characterisation. *Marine and Petroleum Geology* 23: 585-604.
- Hampton, M.A., Lee, H.J. & Locat, J.**, 1996. Submarine landslides. *Reviews of Geophysics* 34: 33-59.
- Helland-Hansen, W. & Martinsen, O.J.**, 2008. Shoreline trajectories and sequences; description of variable depositional-dip scenarios. *Journal of Sedimentary Research* 66: 670-688.
- Hunt, D. & Tucker, M.E.**, 1992. Stranded parasequences and the forced regressive wedge systems tract: deposition during base-level fall. *Sedimentary Geology* 81: 1-9.
- Huuse, M.**, 2002. Late Cenozoic palaeogeography of the eastern North Sea Basin: climatic vs tectonic forcing of basin margin uplift and deltaic progradation. *Bulletin of the Geological Society of Denmark* 49: 145-170.
- Huuse, M., Cartwright, J., Gras, R. & Hurst, A.**, 2005. Km-scale sandstone intrusions in the Eocene of the Outer Moray Firth (UK North Sea): migration paths, reservoirs, and potential drilling hazards. In: Doré, A.G. & Vining, B. (eds): *Petroleum Geology: North-West Europe and Global Perspectives - Proceedings of the 6<sup>th</sup> Petroleum Geology Conference*. The Geological Society (London): 1577-1594.
- Huuse, M. & Clausen, O.R.**, 2001. Morphology and origin of major Cenozoic boundaries: eastern Danish North Sea. *Basin Research* 13: 17-41.
- Huuse, M., Lykke-Andersen, H. & Michelsen, O.**, 2001. Cenozoic evolution of the eastern Danish North Sea. *Marine Geology* 177: 243-269.
- Huvenne, V.A.I., Croker, P.F. & Henrief, J.-P.**, 2002. A refreshing 3D view of an ancient sediment collapse and slope failure. *Terra Nova* 14: 33-44.
- Japsen, P. & Bidstrup, T.**, 1999. Quantification of late Cenozoic erosion in Denmark based on sonic data and basin modelling. *Bulletin of the Geological Society of Denmark* 46: 79-99.
- Köthe, A.**, 2007. Cenozoic biostratigraphy from the German North Sea sector (G-11-1 borehole, dinoflagellate cysts, calcareous nannoplankton). *Zeitschrift der Deutschen Gesellschaft für Geowissenschaften* 158: 287-327.
- Köthe, A., Gaedicke, C. & Lutz, R.**, 2008. Erratum: The age of the Mid-Miocene Unconformity (MMU) in the G-11-1 borehole, German North Sea sector. *Zeitschrift der Deutschen Gesellschaft für Geowissenschaften* 159: 687-689.
- Kuhlmann, G.**, 2004. High resolution stratigraphy and paleoenvironmental changes in the southern North Sea during the Neogene. PhD thesis Utrecht University (Utrecht), 205 pp.
- Kuhlmann, G., Langereis, C.G., Munsterman, D., Van Leeuwen, R.J., Verreussel, R., Meulenkamp, J.E. & Wong, T.E.**, 2006. Chronostratigraphy of Late Neogene sediments in the southern North Sea Basin and paleoenvironmental interpretations. *Palaeogeography, Palaeoclimatology, Palaeoecology* 239: 426-455.
- Kuhlmann, G. & Wong, T.E.**, 2008. Pliocene paleoenvironment evolution as interpreted from 3D-seismic data in the southern North Sea, Dutch offshore sector. *Marine and Petroleum Geology* 25: 173-189.
- Laursen, G.V., Konradi, P.B. & Bidstrup, T.**, 1997. Foraminiferal and seismic interpretations of the paleoenvironment of a profile in the Southern North Sea. *Bulletin de la Societe Geologique de France* 168: 187-196.
- Lee, H.J.**, 2009. Timing of occurrence of large submarine landslides on the Atlantic Ocean margin. *Marine Geology* 264: 53-64.
- Leith, W. & Simpson, D.W.**, 1986. Seismic domains within the Gissar-Kokshar seismic zone, Soviet central Asia. *Journal of Geophysical Research* 91: 689-699.
- Leynaud, D., Mienert, J. & Vanneste, M.**, 2009. Submarine mass movements on glaciated and non-glaciated European continental margins: A review of triggering mechanisms and preconditions to failure. *Marine and Petroleum Geology* 26: 618-632.
- Locat, J. & Lee, H.J.**, 2002. Submarine landslides: advances and challenges. *Canadian Geotechnical Journal* 39: 193-212.
- Lucente, C.C. & Pini, G.A.**, 2003. Anatomy and emplacement mechanism of a large submarine slide within a Miocene foredeep in the northern Apennines, Italy: a field perspective. *American Journal of Science* 303: 565-602.

- Martinsen, O.J.**, 1994. Mass movements. *In*: Maltman, A. (ed.): The Geological Deformation of Sediments. Chapman & Hall (London): 127-165.
- Masson, D.G., Harbitz, C.B., Wynn, R.B., Pedersen, G. & Løvholt, F.**, 2005. Submarine landslides: processes, triggers and hazard prediction. *Philosophical Transactions of the Royal Society of London* 364: 2009-2039.
- McGregor, B.A., Rothwell, R.G., Kenyon, N.H. & Twichell, D.C.**, 1993. Salt tectonics and slope failure in an area of salt domes in the northwestern Gulf of Mexico. *In*: Schwab, W.C., Lee, H.J. & Twichell, D.C. (eds): Submarine landslides: selected studies in the U.S. Exclusive Economic Zone. Geological Survey Bulletin: 92-96.
- Micallef, A., Masson, D.G., Berndt, C. & Stow, D.A.V.**, 2007. Submarine spreading: dynamics and development. *In*: Lykousis, V., Sakellariou, D. & Locat, J. (eds): Advances in Natural and Technological Hazards Research: 119-128.
- Michelsen, O., Thomsen, E., Danielsen, M., Heilmann-Clausen, C., Jordt, H. & Laursen, G.V.**, 1998. Cenozoic sequence stratigraphy in the eastern North Sea. *In*: De Graciansky, P.-C., Hardenbol, J., Jacquin, T. & Vail, P.R. (eds): Mesozoic and Cenozoic Sequence Stratigraphy of European Basins. Society for Sedimentary Geology, Special Publications: 91-118.
- Miller, K.G., Kominz, M.A., Browning, J.V., Wright, J.D., Mountain, G.S., Katz, M.E., Sugarman, P.J., Cramer, B.S., Christie-Blick, N. & Pekar, S.F.**, 2005. The Phanerozoic Record of Global Sea-Level. *Science* 310: 1293-1298.
- Mulder, T. & Cochonat, H.P.**, 1996. Classification of offshore mass movements. *Journal of Sedimentary Research* 66: 43-57.
- Munsterman, D.K. & Brinkhuis, H.**, 2004. A Southern North Sea Miocene dinoflagellate cyst zonation. *Netherlands Journal of Geosciences* 83: 267-285.
- Overeem, I., Weltje, G.J., Bishop-Kay, C. & Kroonenberg, S.B.**, 2001. The Late Cenozoic Eridanos delta system in the Southern North Sea Basin: a climate signal in sediment supply? *Basin Research* 13: 293-312.
- Owen, M., Day, S. & Maslin, M.**, 2007. Late Pleistocene submarine mass movements: occurrence and causes. *Quaternary Science Reviews* 26: 958-978.
- Popenoe, P., Schmuck, E.A. & Dillon, W.P.**, 1993. The Cape Fear Landslide: Slope failure associated with salt diapirism and gas hydrate decomposition. *In*: Schwab, W.C., Lee, H.J. & Twichell, D.C. (eds): Submarine landslides: selected studies in the U.S. Exclusive Economic Zone. Geological Survey Bulletin: 40-53.
- Rasmussen, E.S.**, 2004. The interplay between true eustatic sea-level changes, tectonics and climatic changes: what is the dominating factor in sequence formation of the Upper Oligocene - Miocene succession in the eastern North Sea Basin, Denmark. *Global and Planetary Change* 41: 15-30.
- Rasmussen, E.S.**, 2009. Neogene inversion of the Central Graben and Ringkøbing-Fyn High, Denmark. *Tectonophysics* 465: 84-97.
- Sørensen, J.C., Gregersen, U., Breiner, M. & Michelsen, O.**, 1997. High-frequency sequence stratigraphy of Upper Cenozoic deposits in the central and south-eastern North Sea areas. *Marine and Petroleum Geology* 14: 99-123.
- Storvoll, V., Bjørlykke, K. & Mondol, N.H.**, 2005. Velocity-depth trends in Mesozoic and Cenozoic sediment from the Norwegian shelf. *American Association of Petroleum Geologists Bulletin* 89: 359-381.
- Ten Veen, J.H., Mikes, D., Postma, G. & Steel, R.J.**, 2008. Shelf-edge delta architecture resulting from in- and out phase changes in supply and sea-level in ice-house periods. 26<sup>th</sup> Regional Meeting of International Association of Sedimentologists Abstract (IAS).
- Ten Veen, J.H., Van Gessel, S.F. & Den Dulk, M.**, 2012. Thin- and thick-skinned salt tectonics in the Netherlands; a quantitative approach. *Netherlands Journal of Geosciences* 91-4: 447-464, this issue.
- Van Wees, J.D. & Cloetingh, S.A.P.L.**, 1996. 3D flexure and intraplate compression in the North Sea basin. *Tectonophysics* 266: 343-359.
- Ziegler, P.A.**, 1990. Geological Atlas of Western and Central Europe (2<sup>nd</sup> edition). Shell Internationale Petroleum Maatschappij B.V.; Geological Society Publishing House (Bath), 239 pp.